A novel approach for ensemble clustering of colon biopsy images

[a]Saima Rathore, [b]Muhammad Aksam Iftikhar, [c]Mutawarra Hussain, [d]Abdul Jalil
DCIS, Pakistan Institute of Engineering and Applied Sciences, Islamabad, Pakistan
[a]saimarathore_2k6@yahoo.com, [b]aksam.iftikhar@gmail.com, [c]mutawarra@pieas.edu.pk, [d]jalil@pieas.edu.pk

Abstract—Colon cancer diagnosis based on microscopic analysis of biopsy sample is a common medical practice. However, the process is subjective, biased and leads to inter-observer variability. Further, histopathologists have to analyze many biopsy samples per day. Therefore, factors such as tiredness, experience and workload of histopathologists also affect the diagnosis. These shortcomings require a supporting system, which can help the histopathologists in accurately determining cancer. Image segmentation is one of the techniques, which can help in efficiently segregating colon biopsy image into constituent regions, and accurately localizing the cancer. In this work, we propose a novel colon biopsy image segmentation technique, wherein segmentation has been posed as a classification problem. Local binary patterns (LTP), local ternary patters (LTP), and Haralick features are extracted for each pixel of colon biopsy images. Features are reduced using genetic algorithms and F-Score. Reduced features are given as input to random forest, rotation forest, and rotation boost classifiers for segregation of image into normal, malignant and connecting tissues components. The clustering performance has been evaluated using segmentation accuracy and Davies bouldin index (DBI). Performance of classifiers has also been evaluated using receiver operating characteristics (ROC) curves, and area under the curve (AUC). It is observed that rotation boost in combination with F-Score has shown better results in segmenting the images compared to other classifiers.

Keywords- Colon biopsy; Segmentation; LTP, LBP, Haralick

I. INTRODUCTION

Colon is one major constituent of large intestine. Colon cancer causes deaths of about 0.5 million people each year. Major reasons of colon cancer are excessive smoking, increasing age and diets which are, low in fruit/vegetation and high in fat [1]. Cancer is caused by abnormal growth of tissue and turning into colonic polyps. Polyps are usually benign, and show cancer symptoms after 5-6 years of their startup by the time cancer is too late to cure.

Traditionally, colon cancer is diagnosed using microscopic analysis of histopathological tissue samples. Pathologists assign cancer grades to the samples depending upon the deformation of cells that they observe in images. Usually, five stages of colon cancer, 0, A-D, are assigned using Duke's scale [2,3]. The starting stage is identified by stage 0 in which cancer has just started to develop and tissues are still coherent, whereas D is the final cancer stage in which cancer has reached other body parts such as lungs, liver etc. In stage D, colon tissues are poorly deformed, unstructured and have almost amorphous shape.

Microscopic inspection of biopsy samples is time-consuming and laborious task for the histopathologists, and leads to significant inter-observer variation in grading [4,5]. Heterogeneity of features in some regions also adds to the delicacy of the diagnostic process. Such problems become critical if the results of the biopsy sample are to be used for deciding treatment plans. Therefore, automatic colon cancer detection techniques are in high demand.

A computer-aided diagnosis system for colon biopsy images generally comprises two stages. First, the input image is segregated into biologically different constituent regions. Next, the individual regions are classified into normal and malignant tissues. The scope of this research work is the development of a novel technique for colon biopsy image segmentation.

Segmentation of colon biopsy images is an extremely challenging task owing to similar color intensities in normal and malignant regions of the images. The problem is alleviated by incorporating information about organization of normal and malignant colon tissues into the segmentation process. Several methods have been proposed in this context, which are summarized in a recently reported survey by Rathore et al. [6]. In 2004, Rajpoot et al. proposed a wavelet based technique for segmentation of colon biopsy images [7]. In 2009, Tosun et al. proposed an object oriented texture analysis based technique, called object oriented segmentation (OOSEG), for segmentation of colon biopsy images [8]. In this work, image is divided into three clusters, namely white, pink and purple clusters corresponding to epithelial cells, connecting tissues and lumen. Circular primitives are extracted from each cluster, and then based on certain textural features, initial seeds (regions) are determined. Regions are grown in successive iterations until they span the entire image. Finally, based on certain features of the regions final region boundaries are identified in region merging phase.

Demir et al. further extended the idea proposed by Tosun et al. but in a different direction [9]. Primitives are found using previous work [8]. These primitives are used to construct an object graph, wherein primitives act as nodes and links depend upon primitive types at the end of the links. For each lumen object L, various features are extracted by considering neighbors within a circular window around it. These features are further used by the k-means algorithm to segregate lumen objects into 'gland' and 'non-gland' classes. Lumen objects belonging to 'gland' class are treated as initial seeds. Region growing process involves another object graph which is constructed by considering the nucleus objects as nodes, and assigning edges between each node and its predefined closest nodes. Starting from the initial seeds, regions are then grown

978-1-4799-2293-2/13 $31.00 © 2013 IEEE
DOI 10.1109/FIT.2013.12

until a graph edge is encountered (a pixel that is located on an edge is found). The proposed approach uses the nucleus object graph edges rather than nucleus pixels to stop region growing.

Later, Tosun et al. proposed another interesting method [10] of colon biopsy image segmentation, wherein the object graph is created in a similar fashion as done in [9]. Graph run-length matrices of primitives are calculated for identifying initial regions. Different regions comprise circles, instead of pixels as in [9]. Regions are grown and merged in successive iterations. In the end, Delaunay triangulation is used to convert the primitives based regions into pixel based regions.

Simsek et al. introduced a new feature type, namely co-occurrence features to define spatial relationship between circular primitives in the colon biopsy image [11]. The object graph is created in a similar fashion as in [9,10]. Co-occurrence matrix is calculated for each node of the graph, and 24 co-occurrence features are extracted from the matrix. In this work, segmentation has been posed as a graph partitioning problem. Dissimilar objects are picked in different iterations to generate different graphs. Segmentation is achieved by using these diverse graphs. Finally, multiple segmentation results are combined to obtain final segmentation. Rathore et al. modified the OOSEG technique and used elliptic primitives instead of circular ones in order to locate epithelial cells [12]. GA is employed to find optimal values of different parameters such as radius of window, merge threshold, and optimal length of semi-major and semi-minor axis of ellipse. Further, a member ship function is introduced to find near elliptic shapes along with elliptic ones. This scheme has proven to be effective for images captured at different magnification factors.

However, these techniques suffer a few drawbacks. First, they are computationally very expensive. Locating primitives in three image clusters is computationally expensive, and consumes considerable CPU time. Likewise, region growing and merging processes need calculation of features for updated regions in every iteration. Second, most of these techniques have been designed for images captured at a particular magnification factors, and cannot perform well at other magnification factors. Third, a few of these techniques require manual adjustment of system parameters.

In this research, we propose a novel colon biopsy image segmentation technique. The proposed technique is simple and straightforward. It not only shows its supremacy in terms of segmentation accuracy, but is computationally tractable. In the proposed technique, LBP, LTP and Haralick features are extracted for each image pixel. Features are overwhelmingly large in size which cause computational overload. Therefore, features are reduced using two standard approaches; genetic algorithm and F-Score. Reduced features are then employed to cluster colon biopsy images into biologically different regions (normal, malignant, connecting tissues). Three clustering algorithms, namely random forest, rotation forest, and rotation boost have been employed for classification.

The rest of the paper is organized as follows. Section II presents the proposed methodology. Section III provides experimental results, and Section IV concludes the paper.

II. PROPOSED METHODOLOGY

The proposed technique comprises five phases, namely (1) pre-processing, (2) feature extraction, (3) feature selection, (4) clustering of colon biopsy images, and finally, (5) post-processing. Top-level layout of the proposed technique is given in Figure 1, and subsequent text explains these phases.

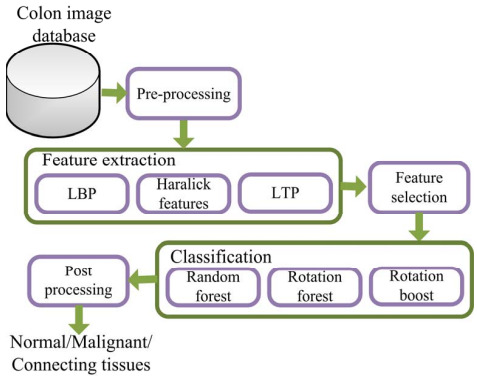

Figure 1: Schematic of the proposed technique

A. *Preprocessing*

Pre-processing step is usually performed in order to make the dataset suitable for further processing. Colon biopsy images may have slight degradation in contrast due to staining artifacts or unbalanced microscopic equipment. Therefore, we have enhanced the contrast of the given images in preprocessing step to tackle the aforementioned issues.

B. *Feature extraction*

Clustering algorithms, where clustering is posed as a classification problem, usually require features corresponding to each image pixel. Therefore, the main purpose of feature extraction phase is to formulate a feature vector for every pixel in the image. Features are desired to be minimal, and must have good discriminating power. In this research work, three different types of features, namely LTP, LBP and Haralick features are extracted. The extracted features are combined for use in clustering of colon biopsy images. These features have been explained in the following text:

- Local binary patterns (LBP)
  LBPs were proposed by Ojala et al. [13]. It is a texture based feature extraction strategy for gray-level patterns in an image. LBPs evaluate the binary differences between the gray-level of central pixel *c,* and P pixels in its neighborhood on a circle of radius R. The method of obtaining LBP code is in Figure 2.

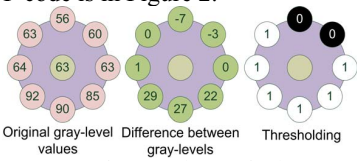

Figure 2: LBP code generation mechanism

The LBP code is generated using Equation (1).

$$LBP_{P,R} = \sum_{p=0}^{P-1} f(v_p - v_c)2^p \quad (1)$$

Where v_p and v_c, respectively, represent gray-level values of p^{th} neighbor and the central pixel c. The function $f(p)$ is a threshold function as given below;

$$f(p) = \begin{cases} 1, \ if \ \ v_p - v_c \geq 0 \\ 0, \ otherwise \end{cases} \quad (2)$$

LBP code for the example given in Figure 2 is;

$LBP = 1*2^0+1*2^1+1*2^2+1*2^3+1*2^4+1*2^5+0*2^6+0*2^7 = 63$

In this work, LBP codes have been generated using uniform rotation invariant mapping (see [13]) by considering eight adjacent neighbors (P=8 and R=1).

- Local ternary patterns (LTPs)

  LTPs are based on the generalization of LBPs [14]. In LTPs, the difference between a central pixel c and its neighbor p is based upon a ternary value according to a threshold θ. LTPs are calculated as follows;

$$f(p)=\begin{cases}+1 \ , \ if \ \ v_p \geq v_c+\theta \\ -1 \ , \ if \ \ v_p \leq v_c-\theta \\ 0 \ \ , \ otherwise \end{cases} \quad (3)$$

  The procedure of LTP computation is given below:

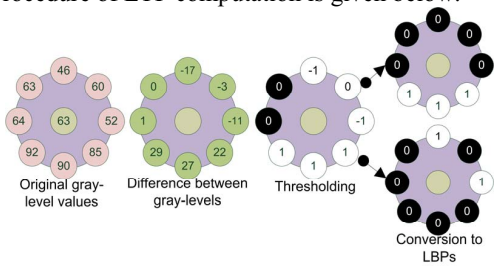

Figure 3: LTP code generation mechanism

  LTP is split into two binary patterns depending upon its positive and negative components as shown in Figure 3. The histograms computed from the two binary patterns are concatenated to obtain the feature vector for LTP. In this study, LTP codes have also been generated using uniform rotation invariant mapping by considering eight adjacent neighbors with $\theta = 10$.

- Haralick texture patterns

  Haralick texture features [15] were proposed by Haralick in 1979. These are texture based statistical features, which have been exploited in various research studies [16,17] for classification. For Haralick feature extraction, a rectangular window is assumed around each image pixel, and a spatial gray level dependence matrix (SGLD) of size NxN is obtained for the image patch. N is the quantization level into which all intensity values are quantized. SGLD matrix is calculated for various combinations of angle θ and distance d (measured in no. of pixels).

  In current work, we have used N=8, d=1, and θ=0°, 45°, 90°, 135°. Eleven statistical measures have been calculated from each SGLD matrix, namely energy, correlation, inertia, entropy, inverse difference moment, sum average, sum variance, sum entropy, difference average, difference variance, and difference entropy. As a result, we have obtained 44 features for each image pixel.

C. *Feature selection*

High dimensional/irrelevant features require more computational time and resources, therefore, meaningful features may be selected from the feature vector to achieve better performance in terms of accuracy and computational time. Many search procedures have been proposed for feature selection. Here, we have reduced feature set by two methods.

First, we used the WEKA, a machine learning tool, to obtain the optimized features using genetic search method. Second, the features have been reduced using F-Score method, which strives to minimize the within class distance and maximize the between class distance. This method selects features based on the F-Score computed for each feature. F-Score of the k^{th} feature is computed using Equation (4).

$$FScore_k = \frac{(\mu_1(k)-\mu(k))^2+(\mu_2(k)-\mu(k))^2}{\frac{1}{P-1}\sum_{n=1}^{P}(\mathbf{P}_n(k)-\mu_1(k))^2+\frac{1}{Q-1}\sum_{m=1}^{Q}(\mathbf{Q}_m(k)-\mu_2(k))^2} \ ; k=1,2,3,...,K \quad (4)$$

where P and Q are the number of samples of normal and malignant classes, respectively. $\mathbf{P}_n(k)$ and $\mathbf{Q}_m(k)$, respectively, correspond to values of k^{th} features for n^{th} and m^{th} samples of normal and malignant classes. $\mu_1(k)$, $\mu_2(k)$ and $\mu(k)$ are the mean of feature values for normal, malignant and total samples corresponding to k^{th} feature. The larger the F-Score, the more discerning the feature is.

D. *Clustering*

Features selected through genetic search and F-Score are given as input to the classifiers for clustering colon biopsy images. In this work, three ensemble classifiers, namely random forest, rotation forest, and rotation boost have been used.

- Random forest

  In random forest, random features are selected in the training phase, and decision trees are grown on the subsets of features [18]. Final predictions are made by combining the predictions of individual decision trees. The random forest for being combining the output of several individual decision trees substantially improves performance compared to individual decision trees.

- Rotation forest

  Rotation forest is another ensemble classifier that not only caters accuracy of classification but also encourages diversity in training data [19]. Rotation forest employs linear feature extraction methods, like, principal component analysis (PCA), and independent component analysis (ICA) on the input data. Original feature space is divided into N smaller subsets, and PCA or ICA is applied on each smaller subset, thereby resulting in axis rotation and generation of new attributes for the base classifiers. Random forest seeks diversity by employing feature selection strategy, and encourages accuracy by utilizing all the principal components after rotation.

- Rotation boost

  Rotation boost is also an ensemble classifier strategy [20] that is developed by combining rotation matrix concept of rotation forest, and weight updation process of AdaBoost. It is a sequential classifier in which base classifiers are trained by considering the performance of previous base classifier. Initially equal weights are assigned to all the training samples. But, in subsequent iterations, weights are updated in such a way that more weight is given to the samples which are misclassified in previous iteration, and less weight is given to the samples, which are correctly classified by previous classifier. This way, rotation boost tackles hard instances quite intelligently.

E. Post Processing

Clustering phase may over segment the images due to noise or blur present in the images. Post processing phase has been especially designed to overcome this limitation. In this phase, classes of pixels are updated depending upon the classes of its adjacent neighbors. For this purpose, a similarity threshold equal to 75% has been used. It defines that the class of a pixel should be updated to class t, if more than 75% of its adjacent pixels belong to class t. Otherwise, its class is left unchanged.

III. Experimental Results

The features extracted in Section II*C* have been given as input to the classifiers for classification of pixels into normal, malignant and connecting tissues. All the computations have been performed on Intel Core i7, 2.4 GHz processor with 12 GB RAM. 100 RGB images and corresponding ground truth has been used in the experiments. Dataset has been acquired from Rawalpindi Medical College, Pakistan. Images have spatial resolution of 600x800, and are either homogenous (comprising normal or malignant tissue) or heterogeneous (comprising both normal and malignant tissues). The connecting tissues are part of both image types.

Three types of experiments have been conducted on the given dataset. In the first two experiments, OOSEG and GRLM techniques have been tested. Several parameters given in Table I have been adjusted manually for OOSEG and GRLM.

TABLE I. Parameters setting for OOSEG and GRLM

Parameter name	Parameter value
Minimum circle radius	2 pixels
Component area threshold	100 pixels
Merge threshold	1.2
Smaller and larger window sizes	96 pixels and 253 pixels
Size and type of structuring element	2 , Disk

In the third experiment, LTP, LBP and Haralick features have been extracted for each image pixel. Features have been combined to form a hybrid feature vector. In order to reduce the computational complexity and to discover meaningful features, F-Score and genetic search have been employed. Corresponding results have been reported in Table II.

TABLE II. Feature selection through Genetic Search and F-Score

Feature selection through feature selection techniques				
Feature selection technique	***LBP***	***LTP***	***Haralick features***	***LBP+LTP+ Haralick features***
Original features	36	36	44	**116**
Genetic search	28	25	34	**87**
F-Score	19	21	26	**66**

It is observed from Table II that F-Score appears to be a promising method of feature selection for colon biopsy images. F-Score has substantially reduced the total length of combined feature set from 116 to 66, thereby saving computational cost to a great extent. For training and testing phases, 25 and 75 images have been used, respectively. Clustering (segmentation) performance has been measured in terms of two well-known parameters; Davies bouldin index (DBI) and segmentation accuracy (SA). DBI is an internal measure for which the ground truth is not required. Whereas, SA is an external measure which requires ground truth.

DBI: It is the ratio of sum of within class scatter to between classes scatter. It can be calculated using Equation (5).

$$DBI = \frac{1}{N}\sum_{i=1}^{N}\max\left\{\frac{\bar{D}(Q_i)+\bar{D}(Q_j)}{D(Q_i,Q_j)}\right\} \quad (5)$$

where N is the total number of clusters (classes), $D(Q_i,Q_j)$ is the distance between centers of clusters Q_i and Q_j. $\bar{D}_{(Q_i)}$ and $\bar{D}_{(Q_j)}$ are the average distances of points of clusters Q_i and Q_j to their cluster centroids, respectively. DBI will have smaller value if within class scatter is minimum and between classes scatter is maximum. It implies smaller the DBI, better the clustering. Valid values of DBI range from 0 to 1.

SA: It is a measure of effectives of the segmentation technique. It is the ratio between the numbers of pixels, which are correctly classified to the total number of pixels. Valid values of segmentation accuracy range from 0 to 100.

Segmentation performance measured in terms of these two parameters for all feature types is reported in Table III and IV.

TABLE III. Segmentation performance using LBP and LTP features

LBP features						
Feature selection technique	***Random forest***		***Rotation forest***		***Rotation boost***	
	DBI	***Acc (%)***	***DBI***	***Acc (%)***	***DBI***	***Acc (%)***
Original features	0.33	91.0	0.32	91.1	0.30	92.8
Genetic search	0.29	94.0	0.26	94.8	0.22	95.3
F-Score	0.26	94.8	0.25	94.9	0.21	**95.8**
LTP features						
Feature selection technique	***Random forest***		***Rotation forest***		***Rotation boost***	
	DBI	***Acc (%)***	***DBI***	***Acc (%)***	***DBI***	***Acc (%)***
Original features	0.27	94.7	0.22	95.5	0.21	95.8
Genetic search	0.19	97.4	0.15	97.6	0.14	98.0
F-Score	0.16	97.6	0.14	97.8	0.13	**98.2**

TABLE IV. Segmentation performance using Haralick and Hybrid features

Haralick features						
Feature selection technique	***Random forest***		***Rotation forest***		***Rotation boost***	
	DBI	***Acc (%)***	***DBI***	***Acc (%)***	***DBI***	***Acc (%)***
Original features	0.33	90.8	0.33	90.8	0.31	91.7
Genetic search	0.31	93.2	0.30	93.6	0.28	94.1
F-Score	0.29	93.8	0.28	94.0	0.26	**94.5**
LBP+LTP+Haralick features						
Feature selection technique	***Random forest***		***Rotation forest***		***Rotation boost***	
	DBI	***Acc (%)***	***DBI***	***Acc (%)***	***DBI***	***Acc (%)***
Original features	0.22	95.5	0.20	96.2	0.19	96.3
Genetic search	0.15	98.0	0.13	98.4	0.12	98.5
F-Score	0.13	98.5	0.12	98.8	0.10	**98.8**

It is observed from results of Table III and Table IV that LTP features yield promising results for both types of reduced feature sets; selected by F-Score and genetic search. Maximum accuracy using LTP features is 98.2% when rotation boost and F-Score have been used together. Further, it is observed that hybrid features produce superior results compared to individual features. Segmentation accuracy for hybrid features is 98.8%, which is superior compared to individual best of 95.8%, 98.2% and 94.5% for LBP, LTP and Haralick features, respectively. Moreover, rotation boost classifier proves to be a promising solution for challenging problem of colon biopsy image

segmentation compared to other classifiers. Comparing individual feature selection techniques, F-Score based features yield better performance compared to features selected by genetic search. Similar pattern is observed in terms of DBI. DBI of hybrid features is 0.10, which is superior compared to the individual best of 0.21, 0.13, 0.26, respectively, for LBP, LTP and Haralick features.

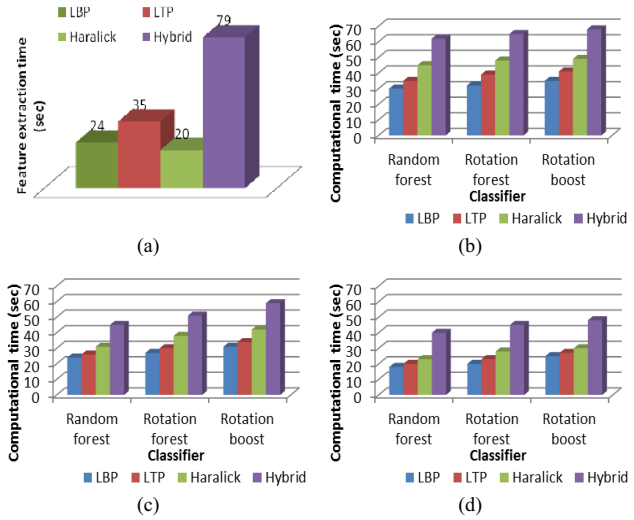

Figure 4: (a) Extraction time, classification time taken by different classifiers for (b) original feature set, feature sets selected by (c) Genetic search (d) F-Score

Figure 4 demonstrates the CPU time taken by different classifiers in classifying original and reduced datasets. Rotation boost classifier takes more time for classification compared to others, however, it maintains better performance. Further, it is observed that F-Score based dataset takes smaller time for classification owing to its smaller size. As far as extraction time of features is concerned, it is observed that extraction of LTP takes more time compared to others.

Performance of the classifiers is also analyzed in terms of ROC curves and area under the curve. ROC curves have been presented in Figure 5 for datasets, selected by genetic search and F-Score. ROC curves also demonstrate the supremacy of Rotation boost classifier over others.

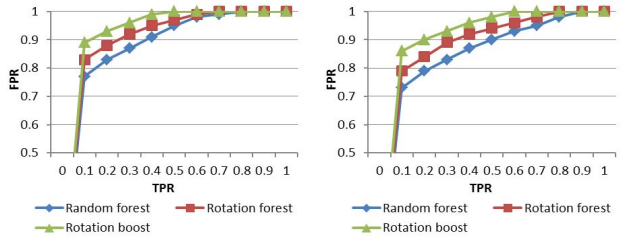

Figure 5: ROC curve of various decision models for feature sets selected by (a) F-Score, and (b) genetic search

Area under the curve (AUC) is another parameter that can be measured from ROC. It is the maximum realizable ROC and has been used in many studies to evaluate the effectiveness of classifiers. In this work, we have also evaluated AUC of ROC curve for each classifier. Rotation boost manages to achieve maximum AUC of 0.98 for feature set selected by F-Score. AUC of different classifiers is given in Figure 6.

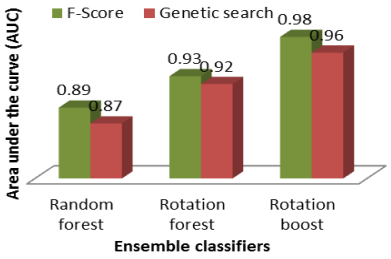

Figure 6: AUC for various classifiers

Visual results of segmentation for a few colon biopsy images are shown in Figure 7. Figure 7 (a1-a3) comprise malignant and connecting tissues. OOSEG and GRLM both suffer in accurately determining the boundary. However, the proposed technique accurately determines the boundary between the two classes. Figure 7 (b1-b3) comprise normal and connecting tissues. OOSEG and GRLM, once again, face difficulty in demarcating boundary between the two tissue types. But, the boundaries demarcated by the proposed technique are well-defined in Figure 7 (b3). Figure 7 (c1-c3) comprises normal, malignant and connecting tissues. The proposed technique has better captured the heterogeneity between different constituents compared to OOSEG and GRLM.

IV. CONCLUSION

In this paper we have proposed a novel colon biopsy image segmentation scheme, wherein segmentation has been posed as a classification problem. F-Score and Rotation boost comes out to be promising feature extraction and classification strategies in order to model the challenging problem of colon biopsy image segmentation. F-Score not only reduces the feature space, but also selects discriminating features which in turn help rotation boost classifier to attain maximum accuracy. The proposed technique attains maximum accuracy of 98.8.% with hybrid features. Analysis reveals that hybrid feature set encompassing diverse information about the image tissue, appear out to be more discriminative compared to individual features. Further, F-Score based features have proven to be more effective compared to genetic search based features with a percentage increase in accuracy of 0.3%, 0.2%, 0.4%, 0.3% for LBP, LTP, Haralick and hybrid features. Therefore, we can hope that the proposed technique can be used as an effective diagnostic tool for the patients of colon cancer. This research can further be extended into two directions. First, making ensemble of classifiers may further improve performance. Second, incorporating other performance evaluation parameters can potentially provide better performance overview.

REFERENCES

[1] "Colon Cancer Risk Factors," http://www.ccalliance.org/colorectal_cancer/riskfactors.html.

[2] M. Fox. "Stages of Colon Adenocarcinoma," http://www.livestrong.com/article/162178-stages-of-colon-adenocarcinoma/.

[3] D. Myers. "Colon Cancer Stages: Basics of Each Colon Cancer Stage," http://coloncancer.about.com/od/stagesandsurvivalrate1/a/ColonCancerStag.htm.

[4] G. D. Thomas, M. F. Dixon, N. C. Smeeton *et al.*, “Observer Variation in the Histological Grading of Rectal Carcinoma,” Journal of Clinical pathology, vol. 36, no. 4, pp. 385-391, 1983.

[5] A. Andrion, C. Magnani, P. G. Betta *et al.*, “Malignant Mesothelioma of the Pleura: Inter Observer Variability,” Journal of Clinical pathology, vol. 48, pp. 856-860, 1995.

[6] S. Rathore, M. Hussain, A. Ali, A. Khan, "A recent survey on colon cancer detection techniques," IEEE/ACM Transactions on Computational Biology and Bioinformatics, 2013.

[7] K. M. Rajpoot and N. M. Rajpoot, "Wavelet Based Segmentation of Hyperspectral Colon Tissue Imagery," Proceedings of 7th Multitopic Conference, pp. 38-43, 2003.

[8] A. B. Tosun, M. Kandemir, C. Sokmensuer *et al.*, “Object-Oriented Texture Analysis for the Unsupervised Segmentation of Biopsy Images,” Journal of Pattern Recognition, vol. 42, pp. 1104-1112, 2009.

[9] C. G. Demir, M. Kandemir, A. B. Tosun *et al.*, “Automatic Segmentation of Colon Glands Using Object-Graphs,” Medical Image Analysis, vol. 14, no. 1, pp. 01-12, 2010.

[10] A. B. Tosun and C. G. Demir, “Graph Run-Length Matrices for Histopathological Image Segmentation,” IEEE Transactions on Medical Imaging, vol. 30, no. 3, pp. 721-732, 2011.

[11] A. C. Simsek, A. B. Tosun, C. Aykanat *et al.*, “Multilevel Segmentation of Histopathological Images Using Cooccurrence of Tissue Objects,” IEEE Transactions on Biomedical Engineering, vol. 59, no. 6, pp. 1681-1690, 2012.

[12] S. Rathore, M. Hussain and A. Khan, "A Novel Approach for Colon Biopsy Image Segmentation" Proceedings of International Conference on Complex Medical Engineering, 2013.

[13] T. Ojala, M. Pietikainen and D. Harwood, “A Comparative Study of Texture Measures with Classification Based on Feature Distribution,” Pattern Recognition, vol. 29, pp. 51-59, 1996.

[14] X. Tan and B. Triggs, "Enhanced Local Texture Feature Sets for Face Recognition under Difficult Lighting Conditions," Proceedings of the 3rd International Conference on Analysis and Modeling of Faces and Gestures, pp. 168-182, 2007.

[15] R. M. Haralick, "Statistical and Structural Approaches to Texture," Proceedings of IEEE, pp. 786-804, 1979.

[16] N. A. Hamilton, R. S. Pantelic, K. Hanson et al., "Automated Sub-Cellular Phenotype Classification: An Introduction and Recent Results," Proceedings of Workshop on Intelligent Systems for Bioinformatics, Australian Computer Society, pp. 67-72, 2006.

[17] L. Nanni, A. Lumini, Y. S. Lin *et al.*, “Fusion of Systems for Automated Cell Phenotype Image Classification,” Expert Systems with Applications, vol. 37, pp. 1556-1562, 2010.

[18] L. B. Statistics and L. Breiman, “Random Forests,” Machine Learning, vol. 45, pp. 05-32, 2001.

[19] J. J. Rodriguez, L. I. Kuncheva and C. J. Alonso, “Rotation Forest: A New Classifier Ensemble Method,” IEEE Tranasctions on Patter Analysis and Machine Intelligence, vol.28, no. 10, pp. 1619-1630, 2006.

[20] C. Zhang and J.Zhang, “Rotboost: A Technqiue for Combining Rotation Forest and Adaboost,” Pattern Recognition Letters, vol. 29, no. 10, pp. 1524-1536, 2008.

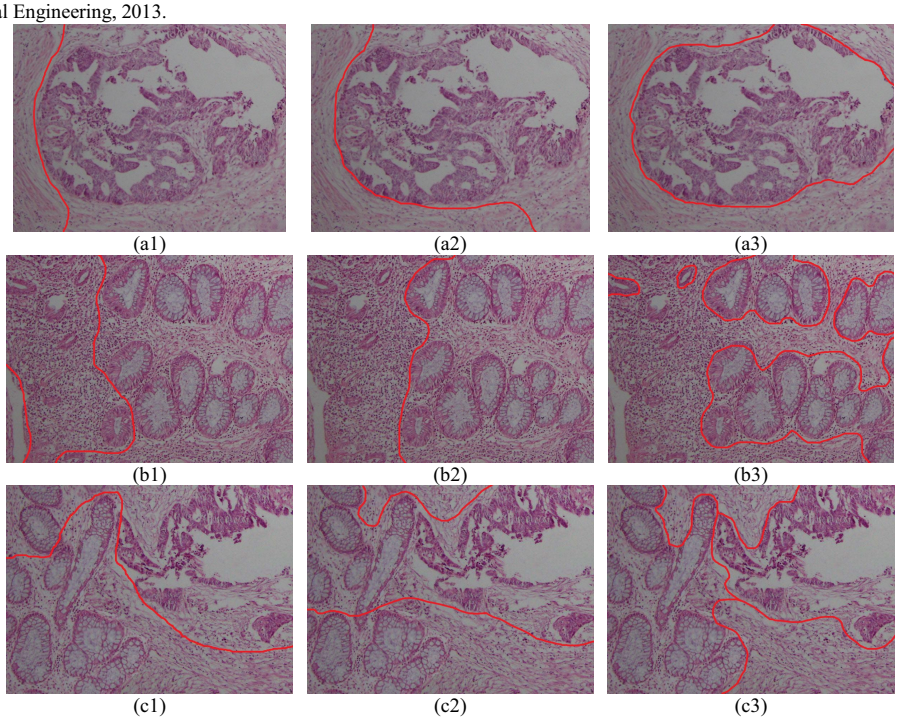

Figure 7: Visual results of segmentation: (a1,b1,c1) OOSEG, (a2,b2,c2) GRLM, and (a3,b3,c3) proposed technique